

Co on Stepped Cu(100) Surfaces: A Comparison of Experimental Data with Monte Carlo Growth Simulations.

S.T. Coyle and M. R. Scheinfein

Dept. of Physics and Astronomy, Arizona State University, Tempe, AZ 85287

James L. Blue

National Institute of Standards and Technology, Gaithersburg, MD 20899

Abstract

Monte Carlo simulations of the growth of Co/Cu(100) in the presence of steps, terraces, and kinks were performed. The beginning stages of Co growth enhance the roughening of step edges. Interdiffusion increases with increasing temperature and decreasing growth rate. Varying the step orientation from $\langle 100 \rangle$ to $\langle 110 \rangle$ produced a steady decrease in interdiffusion. The lateral width of the interdiffused region in steps (10-90% concentration) is $\sim 0.7-1.5$ nm. Decreasing the Co-Cu binding energy produced an increase in the frequency of double-height islands and step edge decoration. A value of ~ 0.21 eV/NN bond produced step edge decoration indicative of a Schwoebel barrier with very few double-height islands. Simulation results were compared to growth results obtained via nanometer resolution ultra-high vacuum scanning electron microscopy. Island statistics compare favorably with growth results. Experimentally observed large etching features at steps were not well reproduced by the model, suggesting an exchange mechanism may be important.

DISTRIBUTION STATEMENT A

Approved for public release;
Distribution Unlimited

19971209 075

To be Published in JVT
(AUS-97)

PACS: 68.35.Ct, 68.55.-a

I. Introduction

Co/Cu(100) has become an important system in the study of thin film magnetism. Face centered cubic (fcc) Co has a small lattice mismatch with fcc Cu(100) and will grow pseudomorphically. Cu surfaces vicinal to $\langle 100 \rangle$ allow Co to be grown with a regularly spaced array of $\langle 110 \rangle$ steps and $\langle 100 \rangle$ terraces¹. Bulk Co and Cu are considered immiscible below ~ 900 K, however, Co and Cu have been reported to form an alloy² above ~ 450 K, and interdiffusion during growth above 0 C has been suggested³. Co/Cu multilayers exhibit giant magnetoresistance, therefore, understanding the Co/Cu interface is important.

We have performed a study of the growth and magnetic properties of Co/Cu(100) at room temperature (RT)⁴ in an attempt to understand how morphology and defects affect film growth and magnetic properties. We described two growth modes: island growth and exchange mediated growth, and reported a continuum of combinations of these two modes in different films. Island growth mode is characterized by the formation of islands on terraces and little interaction with steps, while exchange mediated growth is characterized by little island formation and a high degree of roughening of step edges. A Co adatom moves along a Cu step until it is pinned by a kink, thereby lowering the free energy. Because Co has a higher free energy^{5, 6} than Cu, the configurational energy may be lowered when Cu atoms move to surround the Co atom. This results in a restructuring of the step edge resulting in faceting along the lower energy $\langle 110 \rangle$ directions. Incorporation into a $\langle 110 \rangle$ step is much more energetically favorable than incorporation into a $\langle 100 \rangle$ step⁴, and this difference may contribute to the difference between island and exchange growth.

We have performed growth simulations using J. L. Blue's kinetic Monte Carlo simulation program⁷ in order to understand the various growth modes encountered during growth experiments. We are also interested in exploring the effects of growth parameters on interdiffusion. Interdiffusion and its affect on magnetic properties at the Co-Cu interface is of central importance in understanding GMR and other thin-film magnetic properties. We attempt to describe the sharpness and character of the interface, and its dependence on parameters such as growth temperature, growth rate, and terrace width.

II. Monte Carlo growth simulations

Kinetic Monte Carlo simulations of the growth of Co on Cu(100) in the presence of step edges were performed. Prior to deposition the Cu substrate was 100 by 100 atoms (square), 6 layers deep, and included one or two terraces with steps oriented along either $\langle 100 \rangle$ or $\langle 110 \rangle$. Simulations were also performed at intermediate step orientations in 5 degree increments. Deposition of Co was simulated at rates of 0.15 ML/min (slow) and 1.5 ML/min (fast), and for coverages between 0.05 ML and 0.50 ML in increments of 0.05 ML. Initial kink densities of 0 and 0.15 kinks per site along the step edges were selected. Substrate temperature during growth was varied from 275 K to 325 K to investigate the effect of temperature on morphology and interdiffusion for RT deposition. Five different simulations were performed with different random number seeds, and the quantitative measures were averaged.

The simulations assumed an Arrhenius-type barrier model, where the transition rate is $r = R_0 \exp(-\epsilon/kT)$. Activation energies (ϵ) were set proportional to beginning and ending bond energies according to $\epsilon = A/(1+|\Delta E|/B) + H(\Delta E)$. The constant A is the energy barrier for hopping to a state of the same energy, and was set to approximate the experimental activation energy for Co adatom diffusion on Co(100)⁸. H is the Heaviside function, T is the substrate temperature, k

is Boltzmann's constant, and B is a constant which reduces the barrier somewhat when the initial and final energies differ. A and B were each set to 0.5 eV. Periodic boundary conditions were employed, with hops allowed along $\langle 110 \rangle$ directions only. The difference in beginning and ending bond energies (ΔE) is found from the sum of all nearest neighbor (NN) and next nearest neighbor (NNN) bond energies before and after the hop. The Co-Co bond energy was 0.271 eV/NN and 0.004 eV/NNN.⁵ The Cu-Cu bond energy was 0.190 eV/NN and 0.003 eV/NNN.⁵ The Co-Cu bond energy was 0.2305 eV/NN and 0.0035 eV/NNN. To our knowledge, the Co-Cu bond energy has not been reported in the literature, we therefore chose a value that is the average of the Co-Co and the Cu-Cu bond energies. We also varied this as a parameter to see its effect on growth.

We have defined a set of measures in order to characterize the effect of various parameters on morphology. Mean island size (S_{av}) is the mean of the distribution of island areas. Island density (N_{av}) is the number of islands per unit area. Interface width (W_i) is calculated as the standard deviation of the surface height distribution in units of a_0 ($a_0=0.361$ nm). This is a measure of the film-vacuum interface roughness. Step width (W_s) is calculated as the standard deviation of the distance of each step edge atom from the center of the terrace. This is a measure of the roughness of the step, also in units of a_0 . Interdiffusion width (W_d) is a measure of the mean width of the interdiffused atoms for each row of atoms perpendicular to a step edge, in units of a_0 . For example, the width is zero for the following arrangement of atoms perpendicular to a $\langle 100 \rangle$ step: Co-Co-Co-Cu-Cu-Cu; while the width is two for: Co-Co-Cu-Co-Cu-Cu. This provides a measure of interdiffusion which is independent of the length and roughness of the step.

III. Results

A. General Effects

The shape, size and density of the islands is essentially the same for simulations with the same deposition rate, independent of step orientation. The islands are approximately rectangular with edges along $\langle 110 \rangle$ directions. Between 30 and 60 percent of the adatoms were captured by terraces, with more being captured during slower growth. Mean island area increases approximately linearly with increasing coverage until approximately 0.4 ML have been deposited, where island capture by steps and the agglomeration of very large islands becomes significant. Island density initially increased, then above 0.15 ML was fairly constant as a function of deposition. Both island density and mean island size were essentially unaffected by initial kink density. Interface width increases approximately linearly with coverage due to the deposition of adatoms and the nucleation of islands. Films grown at 1.5 ML/min have a slightly larger interface width than films grown at 0.15 ML/min due to their higher nucleation density. Interface width is essentially unaffected by initial kink density. Step width of $\langle 100 \rangle$ and $\langle 110 \rangle$ steps are approximately the same and are unaffected by growth rate and initial kink density within the statistical uncertainty. The largest increase in step width occurs between 0 and 0.05 ML of Co deposit. A small amount of Co arriving at a step edge apparently induces a significant amount of restructuring, after which further Co deposition causes only incremental restructuring of the step edge. The addition of initial kinks to the steps did not affect the interdiffusion width. Slow growth produced significantly more interdiffusion than fast growth, with the effect being more pronounced on $\langle 100 \rangle$ steps compared to $\langle 110 \rangle$ steps.

Simulations were also performed on terraces without Co deposition. $\langle 100 \rangle$ steps formed $\langle 110 \rangle$ facets similar to those formed during the Co deposition simulations, however, the step

width was approximately half as large for the equivalent amount of simulation time. $\langle 110 \rangle$ steps formed rectangular inclusions only during simulations that included a nonzero initial kink density. These inclusions were much less deep and wider than those simulated during Co deposition. Co deposition is therefore enhancing the roughening of the step edges.

B. Temperature Effects

Simulations of the initial stages of growth (0.05-0.20 ML) on substrates held at 275 K, 300 K, and 325 K were performed. We chose this temperature range because experiments suggest that in this region interdiffusion begins to become important.^{2, 3} Simulations were performed only for no initial kinks, since kink density was not a significant factor in the simulations described previously.

Mean island area increases linearly from 7 nm^2 at 275 K to 25 nm^2 at 325 K for slow growth on $\langle 100 \rangle$ while the nucleation density decreases from 0.015 nm^{-2} to 0.005 nm^{-2} . For fast growth, the mean island area is about half as large as for slow growth accompanied by a corresponding increase in the island density by a factor of two. This is consistent with increased adatom mobility at higher temperatures. Average island size for growth with $\langle 110 \rangle$ steps does not reflect this trend because the terrace separation is smaller and at high temperatures all adatoms often migrated to the bottom of steps. Thus the mean island size was about 5 nm^2 at all temperatures for both growth rates, while the nucleation density was comparable to that on $\langle 100 \rangle$ at all temperatures.

Interface width decreases slightly with increasing temperature for fast and slow growth proximal to both $\langle 100 \rangle$ and $\langle 110 \rangle$ steps. This is related to the size distribution since islands of smaller size increase the interface width. Step width increased only slightly for increased temperature for $\langle 100 \rangle$ steps. This is consistent with a greater mobility of step edge atoms. The

steps are more free to restructure along $\langle 110 \rangle$ directions in order to lower energy. For $\langle 110 \rangle$ steps, the step edge is in fact becoming more smooth with increasing temperature.

Interdiffusion width increases markedly with increasing temperature (from $\langle 1a_0 \rangle$ to $\langle 5a_0 \rangle$). The effect is more pronounced for slow growth, which is again consistent with increased mobility. Interdiffusion is approximately the same for $\langle 100 \rangle$ and $\langle 110 \rangle$ steps at RT, however, at higher temperature is larger for $\langle 100 \rangle$. Initial kink density appears to have no significant effect on interdiffusion. In the simulations for 0.15 ML/min at 325 K with steps along $\langle 110 \rangle$ all of the Co has attached to step edges (no islands). The average width of the transition from pure Co to pure Cu (interdiffusion width) is $5a_0$, or ~ 1.8 nm. The average width of the Co region along the step is ~ 3 nm, therefore over half of the Co atoms in this simulation could be considered to be in a surface alloy phase. If we continued growth to 1.7 ML (the ferromagnetic transition), assuming no further interdiffusion, this would represent about 7% of the Co atoms. This number would decrease with increasing terrace width. It would, however, increase significantly with the inclusion of step bands, which have a high step density. We have simulated step bands by including a trough in the Cu substrate, and find that the level of interdiffusion in the troughs is even higher than that at steps. While the actual percentage of interdiffused atoms will depend on step and step band density, it is clear that an increase in temperature of 50 C can produce a significant increase in interdiffusion and perhaps a significant surface alloy phase.

We have also simulated Co growth near a trough of 1 ML at RT followed by several seconds of annealing at 300 and 350 K. Annealing at 300 K did not have a significant effect, however, annealing at 350 K for 10 seconds resulted in a single layer of Cu covering approximately 2/3 of the Co. The Cu migrated from areas of exposed Cu, leaving behind large vacant areas. This is consistent with experimental results.^{9, 10} The morphology obtained in these

simulations resembles that obtained in our SEM results which exhibit the exchange mediated growth mode.

C. Co-Cu Binding Energy Effects

Because the Co-Cu binding energy was not precisely known, it was varied as a parameter to see its effect on film growth morphology. Co-Cu binding energy was varied from 0.17 to 0.29 eV in increments of 0.02 eV. Representative samples are shown in Fig. 1, which include the atomic positions of the top three levels of atoms for Co deposition of 0.20 ML grown with Co-Cu binding energy for 0.17 (a, b) 0.21 (c, d) and 0.25 (e, f) eV/NN bond for $\langle 100 \rangle$ (a, c, e) and $\langle 110 \rangle$ (b, d, f) terraces at 0.15 ML/min with no initial kinks. The most striking effect is the increasing frequency of double-height Co islands with decreasing Co-Cu binding energy. At 0.17 eV/NN bond nearly all Co atoms, including those decorating the step edge, exist in this double-height state. This is reasonable since an atom on the top level of a double height island will be more tightly bound than an atom in a single height island with the same number of NN's.

Quantitative results of previously described measures as a function of Co-Cu binding energy have been compiled in Fig. 2. The mean island size is larger and density smaller for slow growth than fast growth (Fig. 2(a, b)). The mean island size increases with increasing binding energy from 0.17 to 0.21 eV, above which it remains fairly constant. The island density (Fig. 2(c, d)) decreases dramatically between 0.17 and 0.21 eV, then remains fairly constant thereafter. Both of these are consequences of the increase in double-height islands.

The interface and interdiffusion width as a function of Co-Cu binding energy is shown in Fig. 2(e-h). Interface width is highest at low energies due to double-height islands. The dependence of the interdiffusion width on Co-Cu binding energy is quite different for $\langle 100 \rangle$ and $\langle 110 \rangle$ steps. The interdiffusion width for $\langle 100 \rangle$ steps peaks at 0.21 eV. The interdiffusion width

for $\langle 110 \rangle$ steps increases steadily with increasing binding energy. The interdiffusion width for $\langle 110 \rangle$ steps increases at a higher rate for slow growth than fast growth. No other measure reflects such a qualitative difference between the dependence of $\langle 100 \rangle$ and $\langle 110 \rangle$ steps on Co-Cu binding energy.

D. Step Orientation Effects

The orientation of steps in our growth experiments often do not lie entirely along $\langle 100 \rangle$ or $\langle 110 \rangle$, as steps often are pinned by defects. In order to investigate the general orientational dependence of steps, we have simulated the beginning stages of growth for 1.5 ML/min and 0.15 ML/min for orientations between $\langle 100 \rangle$ and $\langle 110 \rangle$ in increments of 5 degrees. The kink density will, by necessity, change with orientation, with the maximum half way between $\langle 100 \rangle$ and $\langle 110 \rangle$. Step width was equal for $\langle 100 \rangle$ and $\langle 110 \rangle$ steps, and was approximately 1/3 smaller for all other orientations. Step width was slightly larger for fast compared to slow growth. Interdiffusion decreases approximately linearly with orientation from a maximum at $\langle 100 \rangle$ to a minimum at $\langle 110 \rangle$. Interdiffusion is larger for slow growth than fast growth. This is consistent with earlier interdiffusion width results. These results tend to rule out the possibility of dramatic morphological changes occurring for intermediate step orientations.

E. Comparison with Growth Experiment

Monte Carlo growth simulations reproduced many features of the island growth mode observed during growth experiments. The faceting of step edges is reproduced, however, the length scale of the facets is smaller in the simulations than in the growth experiments. During growth experiments step bands tend to form arcs between pinning sites, therefore, perfect $\langle 100 \rangle$ or $\langle 110 \rangle$ step edges are not the norm. We do find, however, many small lengths of step edges which are aligned nearly along crystallographic axes. These segments can be compared to

simulation results in order to test the efficacy of the simulations. Fig. 3 includes SEM micrographs (left) and simulation results (right) of RT growth of 0.1, 0.2, and 0.4 ML, all at 0.15 ML/min. White arrows in the micrographs denote the $\langle 100 \rangle$ direction. The step edge parallel to the arrow in Fig. 3(a) shows large scale faceting, on the order of 5-7 nm. Faceting of the step edge in the 0.10 ML simulation (Fig. 3(b)) appears similar although the size of the facets is slightly smaller (2-3 nm). In Fig. 3(d), an island has grown into the step edge in the middle of the right step which produces a feature similar to the facets seen in Fig. 3(c). This could conceivably account for the larger scale faceting observed in the micrographs, however, the islands do not appear to be large enough or rectangular enough to have caused the faceting in either Fig. 3(a) or (c). The irregular shape of the islands in the micrographs is not reproduced by the shape of the islands in the simulations. STM images^{9, 11-13} show islands with similar shapes to those in Fig. 3(a, c, e). Relaxation likely occurs at the edge of islands and at steps. This process is omitted in our simulation model. Addition of this process would change the kinetics and might account for the discrepancy in island shapes.

Fig. 4 includes SEM micrographs (left) and simulation results (right) of growth of 0.1, 0.2, and 0.35 ML, also at 0.15 ML/min. The step edges in the simulations have formed approximately rectangular inclusions, usually in a region with islands close to the step. Areas without these inclusions tend to have a region denuded of islands near the terrace. The missing Co atoms are obviously in the islands near the inclusions. Such a region appears to exist in the vicinity of the arrow in Fig. 4(a), however, the inclusions are much deeper than those in (b). This suggests that an exchange mechanism may be contributing to the restructuring of the step edges. As deposition increases (Fig. 4(c-f)) the size of the inclusions increase, both in the growth and simulation experiments. The growth experiments, however, produce some striking step edge

morphologies, as seen in Fig. 4(c) and (e). These features were not reproduced in the simulations, except perhaps for higher deposition where island capture by the terrace is evidenced. This observation suggests, again, that some exchange process is at work, or perhaps Cu has migrated from this area, thereby forming the inclusion. Clearly the kinetics at steps are more complicated than the barrier model in our simulation produces. The surface in Fig. 4(c) is an example of the exchange growth mode described previously⁴. Islands are quite rare and step edge restructuring tends to be more pronounced than in surfaces exhibiting the island growth mode. This morphology has not been reproduced in the corresponding simulations.

A comparison of island statistics for growth experiments exhibiting the island growth mode with simulation results is presented in Fig. 5. Mean island size (a), island density (b), and the percent of the surface covered by islands (c) is shown as a function of deposit. The smaller symbols represent simulation results and the larger symbols represent growth experiment results. Each growth data point represents the mean value obtained by analyzing several micrographs taken in different areas of the sample. The error bars represent one standard deviation. SEM micrographs selected for analysis included single height steps with a similar step length to surface area ratio as in the simulations. The simulation data represent 0.15 ML/min growth near $\langle 100 \rangle$ and $\langle 110 \rangle$ step edges with no initial kinks. The percent of the surface covered is reproduced well by the simulations, while island density is slightly higher and mean island area is lower in the simulation experiments than in the growth experiments.

In Fig. 4(c, e) and in many micrographs not shown, bright regions are evident along some of the step edges, indicating that some step edge decoration has occurred. For Co-Cu binding energy near 0.21 eV there is a significant amount of step edge decoration with a small number of double height islands. The step edge decoration tends to be as deep as the Co adsorption region at

the terrace level, since the lower Co-Cu binding energy favors Co-Co bonds. While we cannot precisely determine the Co-Cu binding energy from these experiments, we can say that it is probably greater than 0.19 eV/NN bond based on the island density and lack of double-height islands. Another possible explanation for the step edge decoration is the existence of a Schwoebel barrier¹⁴, that is an additional barrier to hops down over a step edge. These simulation results indicate that for heteroepitaxial systems such a barrier may, in fact, be the result of a particular ratio of binding energies rather than a separate effect.

IV. Conclusion

We have performed Monte Carlo growth simulations of the growth of Co/Cu(100) in the presence of steps, terraces, and kinks. These experiments were not intended to study Co/Cu(100) growth from first principles, rather we were looking to answer specific questions relating to our experimental results. Simulation results for systems with and without Co growth have confirmed that the beginning stages of Co growth accelerate the faceting of $\langle 100 \rangle$ steps along $\langle 110 \rangle$ directions, and promote faceting of $\langle 110 \rangle$ steps, also along $\langle 110 \rangle$ directions. We believe this is driven by surface free energies: first by Cu moving to lower the number of dangling Co bonds, then by restructuring of the step edge to facets along the lowest energy face ($\langle 110 \rangle$). The size of the faceted features observed in growth experiments was often significantly larger than those observed in simulation experiments. Larger scale facets were observed in simulations of annealed surfaces. This suggests that the model does not well reproduce the kinetics at steps, and could probably be improved upon with more realistic barrier heights.

Interdiffusion is essentially complete by 0.20 ML deposition. Interdiffusion increases with increasing temperature and decreasing growth rate, consistent with more time for atoms to rearrange positions between subsequent adatom arrival. Interdiffusion increased with increasing

Co-Cu binding energy. Presumably because these Co-Cu bonds are more difficult to break and thus the rate at which they break decreases. Varying the step orientation from $\langle 100 \rangle$ to $\langle 110 \rangle$ in small increments produced a steady decrease in interdiffusion. This result may be important for the magnetism of vicinal (100) surfaces which have regularly spaced $\langle 110 \rangle$ steps only,¹ and thus would have a minimum amount of interdiffusion for a given step density. It is clear that the interface between Co and Cu is not sharp on an atomic scale: the width of the interdiffusion region (10-90% concentration) is approximately 0.7-1.5 nm. For growth at 0.15 ML/min there is approximately one interdiffused atom for every two unit cells (~ 0.7 nm) along the length of an average step. Interdiffusion, therefore, is highly dependent on step density (terrace width).

Island size and density compare favorably with growth results for the island growth mode, and the effects of deposition rate and temperature are consistent with accepted kinetic models. Island shapes are not well reproduced. Many of the features observed in the exchange mediated growth mode suggest an etching of the step rather than a simple restructuring along $\langle 110 \rangle$ facets. This morphology was duplicated somewhat during annealing simulations. We believe the discrepancy between growth experiments and simulation experiments is due to kinetics. The barrier height model employed in our simulations works well for nucleation and growth of islands, however, the kinetics at steps is more complicated. One or more processes at steps must occur at much different rates than predicted by our model. One possible example is adatom diffusion along a step, which evidence suggests¹⁵ may have a lower activation energy than adatom diffusion across a terrace. The most promising method to improve the simulation results would be to use a complete set of barrier height calculations. This may allow the determination of exactly which processes are responsible for the etching features we observed.

Acknowledgments

The authors would like to thank Dr. G. G. Hembree for collaboration in the experimental work and a critical reading of this manuscript. This work is supported by ONR under grant No. N00014-93-1-0099.

References

- 1 A. Berger, U. Linke, and H. P. Oepen, *Phys. Rev. Lett.* **68**, 839 (1992).
- 2 M. T. Kief, G. J. Mankey, and R. F. Willis, *J. Appl. Phys.* **10**, 5929 (1991).
- 3 J. Shen, R. Skomski, M. Klaua, *et al.*, *Phys. Rev. B* **56**, 2340 (1997).
- 4 S. T. Coyle, G. G. Hembree, M. R. Scheinfein, *J. Vac. Sci. Technol. A* **15**, 1785 (1997).
- 5 L. Z. Mezey and J. Giber, *Jpn. J. Appl. Phys.* **21**, 1569 (1982).
- 6 Y. W. Lee, K. C. Russell, and H. I. Aaronson, *Scr. Metall.* **15**, 723 (1981).
- 7 J. L. Blue, to be published.
- 8 M. T. Kief and W. F. Egelhoff Jr., *Phys. Rev. B* **47**, 785 (1992).
- 9 A. K. Schmid, D. Atlan and H. Itoh, *et al.*, *Phys. Rev. B* **48**, 2855 (1993).
- 10 M. Giesen, F. Schmitz, and H. Ibach, *Surf. Sci.* **336**, 69 (1995).
- 11 U. Ramsperger, A. Vaterlaus, and D. Pescia, *Phys. Rev. B* **53**, 1 (1996).
- 12 A. K. Schmid and J. Kirschner, *Ultramicroscopy* **42**, 483 (1992).
- 13 R. Allenspach, A. Bischof, and U. Durig, *Surf. Sci. Lett.* **381**, L573 (1997).
- 14 R. L. Schwoebel, *J. Appl. Phys.* **40**, 614 (1969).
- 15 P. Stoltze, *J. Phys. Condens. Matter* **6**, 495 (1994).

Figure Captions

FIG. 1: Simulation results for Co deposition of 0.20 ML at 0.15 ML/min in the presence of $\langle 100 \rangle$ (a, c, e) and $\langle 110 \rangle$ (b, d, f) terraces for Co/Cu NN binding energies of 0.17, 0.21, and 0.25 eV/NN bond.

FIG 2: Mean island size (s_{av})(a, b), island density (N_{av})(c, d), interface width (W_i)(e, f), and interdiffusion width (W_d)(g, h) as a function of Co/Cu binding energy for 0.20 ML of deposited Co for terraces with steps oriented along $\langle 100 \rangle$ (a, c, e, f) and $\langle 110 \rangle$ (b, d, f, h). Each graph includes plots of growth at 1.5 and 0.15 ML/min with initial kink densities of 0 kinks/site.

FIG. 3: Comparison of SEM micrographs with simulation results for 0.1 ML (a, b), 0.2 ML (d) and 0.4 ML (e, f) depositions with step edges aligned along $\langle 100 \rangle$. Arrows denote $\langle 100 \rangle$ directions. Growth rate was 0.15 ML/min for all.

FIG. 4. Comparison of SEM micrographs with simulation results for 0.1 ML (a, b), 0.2 ML (c, d) and 0.35 ML (e, f) depositions with step edges aligned along $\langle 110 \rangle$. Arrows denote $\langle 110 \rangle$ directions. Growth rate was 0.15 ML/min for all.

FIG. 5. Comparison of mean island size (s_{av})(a), island density (N_{av})(b), and the percent of the surface covered by islands (θ_{isl})(c) as a function of Co deposit between simulation experiments and growth experiments. Growth experiment data was measured in regions with step densities similar to the simulations. Growth rate was 0.15 ML/min for all.

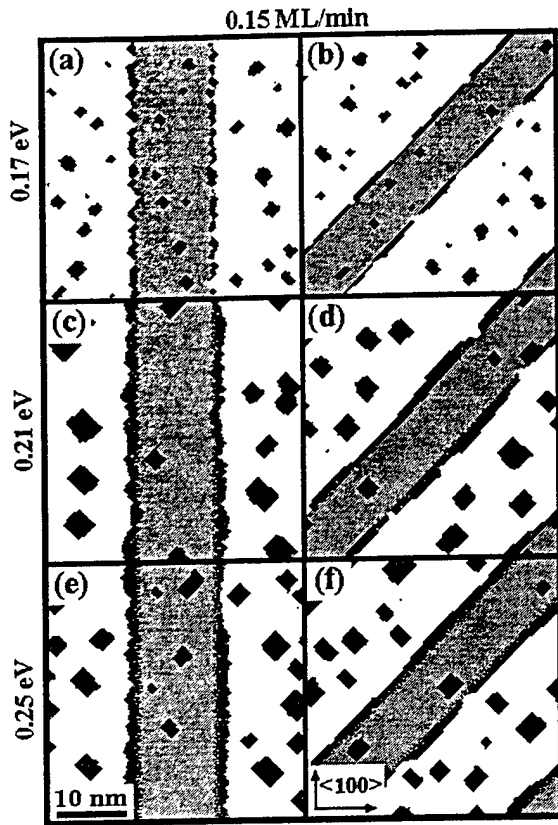


FIG. 1.

Coyle, et al.

JVST

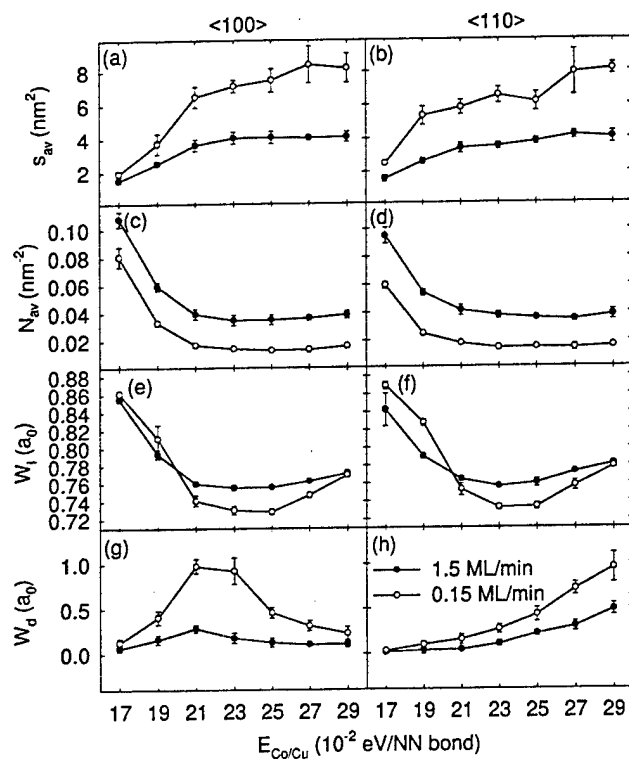


FIG 2.

Coyle, et al.

JVST

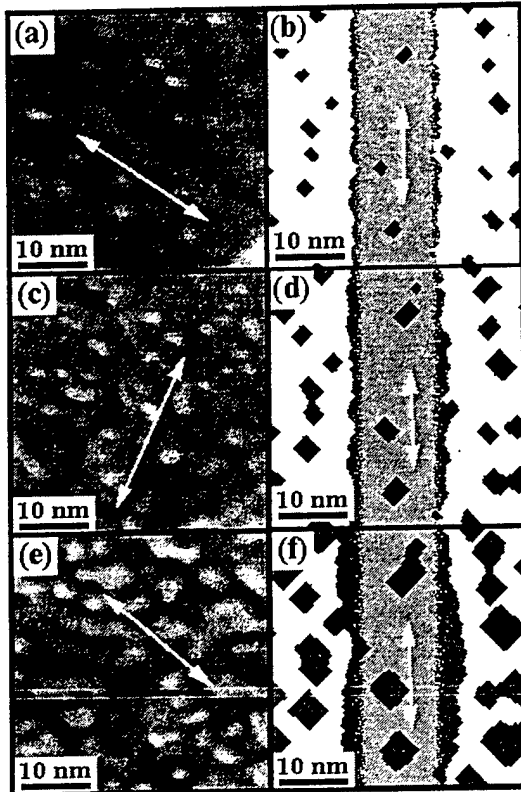


FIG. 3.

Coyle, et al.

JVST

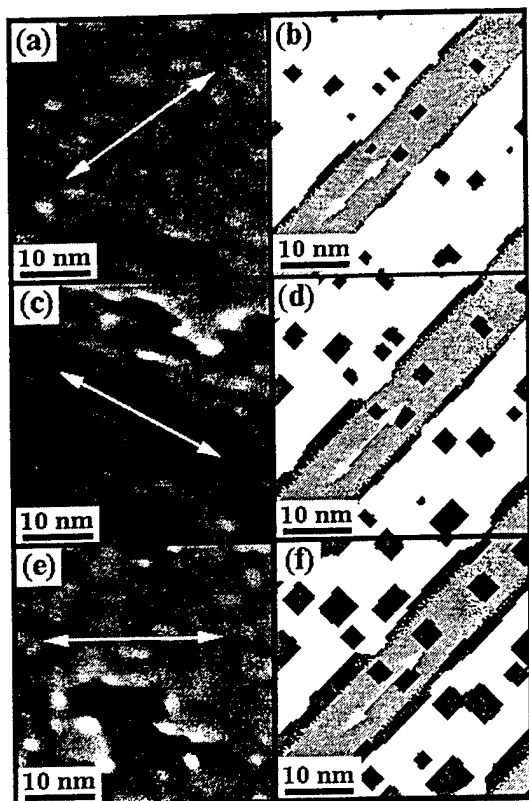


FIG. 4

Coyle, et al.

JVST

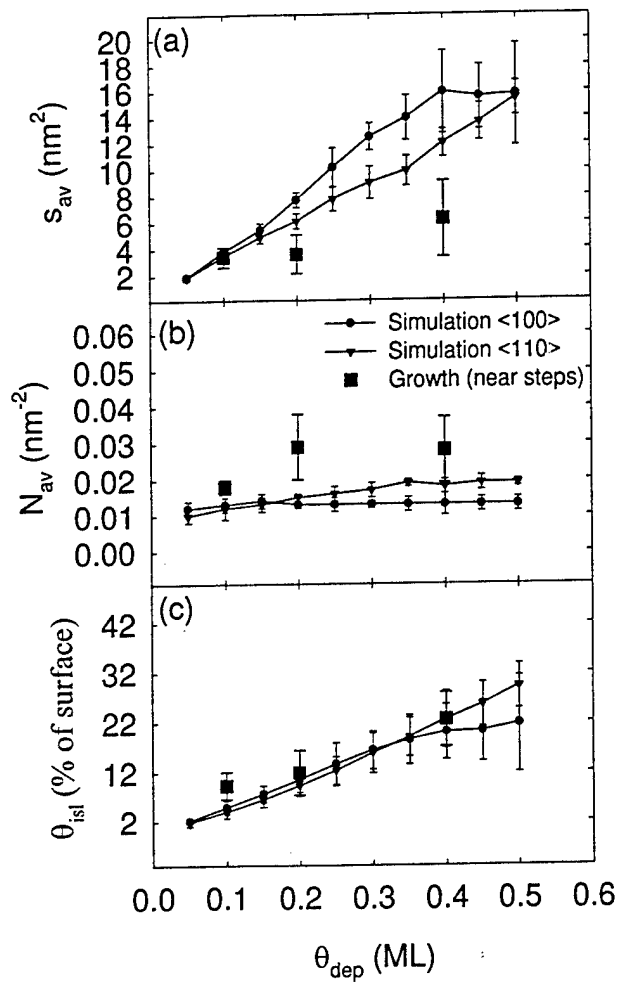


FIG. 5

Coyle, et al.

JVST